Wasit Journal of Engineering Sciences
Journal homepage: https://ejuow.uowasit.edu.iq
ISSN 2305-6932
Original Research
Vol. 14 No. 2 June 2026, pp.415-423
https://doi.org/10.31185/ejuow.v14i2.919

Extraction of high purity Nano-silicon from Quartz Sand by Metallothermic-reduction technique

Ruaa A. Salman[1], Asaad H. Lafta[2]
[1] College of Biomedical Engineering, University of Technology-Iraq
[2] College of Production Engineering and Metallurgy, University of Technology-Iraq

Corresponding Author Email: 70153@uotechnology.edu.iq.

Received Mar.19, 2026 Revised May.9, 2026 Accepted May.11, 2026 Online Jun.1, 2026

ABSTRACT

This study presents an improved approach for extracting high-purity silicon nanoparticles using an enhanced thermal magnesium-aluminum reduction methodology. It lays the foundation for a systematic understanding and transformation of silicon, converting silica (SiO_2) particles into nanosilicon using an optimized aluminum-magnesium mixture for low-temperature silica reduction (a note of low-impact reduction) through a unique chemical treatment. The study employed a protocol of leaching with 4 N HCl followed by treatment with 2.5NNaOH. This was followed by reduction with an aluminum-magnesium mixture, and then a unique chemical treatment involving synergistic leaching and etching of the silicon nanoparticles, along with revitalization etching using a mixture of hydrofluoric and acetic acids. Using this protocol, high-purity silicon nanoparticles with interconnected porous networks were obtained after the complete removal of residual impurities (including methyl green, silicate residues, and other contaminants). Characterization techniques have confirmed the integrated nature of the structure and form of the extracted silicon. All the products were characterized using a field emission scanning electron microscope (FE-SEM), energy dispersive spectroscopy (EDS/EDX), and x-ray diffraction (XRD). Nanosilicon produced by the synthesis method had an average diameter of 49.8625 nm, 30.155 nm, and 58.635 nm, and were calculated from three different sets of samples, based upon the Mg, Al: SiO_2 weight ratios (S1 (35, 65):1, S2 (50, 50):1, S3 (70, 30):1) used to prepare the mixtures for extraction. Also, the XRD and FT-IR results confirm the high purity of the produced nanosilicon nanoparticles. Despite current challenges associated with producing large quantities of porous silicon nanomaterials using metallothermic reduction (MTR) technology, the modified thermochemical method offers a scalable, low-cost, high-throughput approach to manufacturing advanced silicon-based nanomaterials.

Keywords: Porous Silicon, Magnesiothermic Reduction, Chemical Leaching, Nanoparticles, Acid Etching.

1. Introduction

The second most prevalent element found in Earth's crust, silicon (Si) has provided the impetus for fundamental changes in the technology landscape for many industries, including microelectronics and alternative energy. As such, interest in nanostructured porous silicon (PSi) has grown tremendously within both the academic and industrial arenas over the past several years. This growth has been driven by the unique properties of PSi, including its large specific surface area, tunable pore size, and excellent biocompatibility [1-6]. These important features provide Si nanoparticles (SiNPs) with the potential to serve as next-generation materials for high-capacity anodes in lithium-ion batteries (LIBs) due to their theoretical capacitance of approximately 4200 mAh/g, almost 10 times greater than the existing graphite anodes [2,7]. Beyond applications related to energy storage, PSi has revealed considerable potential for use in targeted drug delivery systems, gas sensors, and as a green medium for hydrogen fuel production [8-12]. There are two main pathways for the synthesis of PSi: Electrochemical Etching (ECE) and Metal-Assisted Chemical Etching (MACET). While ECE can provide precise control over pore morphology, the general lack of scalability caused by the high operating costs and

hazardous hydrofluoric acid (HF) concentrations limit its use for producing SiNPs at an industrial level [13-15]. Conversely, Chemical Vapor Deposition (CVD), while producing high-purity SiNPs using energy-hungry processes, require very expensive precursors such as silane (SiH_4) to function [6]. One of the most disruptive developments in creating PSi is the introduction of metallothermic reduction, which allows for the production of functional Si nanostructures from low-cost, naturally occurring silica (SiO_2) sources such as mineral sand, rice husk ash and sol-gel derived materials at relatively low reaction temperatures [15-17].The conventional means of determining thermodynamic feasibility for these reduction reactions employs the famous Ellingham diagram which ranks the affinity of metals to bind to oxygen. Metals such as lithium (Li), sodium (Na), calcium (Ca), magnesium (Mg), and aluminum (Al) have a more negative Gibbs free energy of oxidation than silicon suggesting they could act as reductants in theory; however, practical utilization of the alkali metals (Li, Na) has been greatly limited due to their extremely high reactivity to moisture and the extremely high cost associated with extracting pure metal [17-21]. Currently, magnesiothermic reduction at 650°C is most commonly documented in the literature for its ability to maintain the morphology of the precursor material; aluminothermic reduction can accomplish this faster but often requires higher temperature to initiate the reduction [22-27]. A further critical issue in the present literature is the lack of a fundamental comparative study that examines the influence of various metallic reductants and their binary mixtures on the intrinsic physical properties of resulting Psi [28, 29]. The performance of Si-based devices such as Li^+ ion diffusion kinetics in batteries and release rates from pharmaceutical ingredients are dictated exclusively by the void volume and surface energy of the nanostructures so understanding the "reductant-structure" relationship is vital to this research [30]. For example, previous studies have indicated that amorphous SiNPs are better candidates than crystalline SiNPs in solar cell substrates; however, the conditions needed to stabilize these amorphous phases during thermal reduction have not been optimally defined [30-32]. In this study, we present a novel synthesis route for preparing PSi using Iraqi sand-derived silica nanoparticles as a sustainable precursor. We introduce, for the first time, a binary metallic reductant system (composed of 70% Mg and 30% Al) to support lower reaction threshold and increase specific surface area. This study systematically evaluates how each of these parameters (reaction temperature, reaction time, and the Mg:Al weight ratio) affects subsequent crystallinity, pore volume, and three-dimensional nanostructural arrangement. By creating a bridge between low cost metallurgical methods and highly precise nanotechnology, this work provides a scalable platform for producing high-performance Si for emerging energy and biomedical applications.

2. Materials and methods

2.1. Materials

Raw sand came from the city of Al-Najaf, Iraq (as shown in Table 1 for the chemical analysis of the raw sand). Raw minerals were also acquired from Fluka Co. (Iraq) for use in this study: hydrofluoric acid (HF, 99.6%), acetic acid (CH_2COOH, 98.4%), hydrochloric acid (HCl, 35%) and sodium hydroxide (NaOH, 99.9%). Magnesium and the aluminum powder were supplied by Alfa Co. (Iraq) at an approximate purity of 97.9%.

Table 1. Chemical Composition of Raw Sand.

Material	SiO_2	Al_2O_3	Fe_2O_3	K_2O	TiO_2	Cr_2O_3	H_2O	ZrO_2	Other each
Sand powder	98.05	0.87	0.49	0.08	0.03	0.07	0.34	0.08	0.05

2.2. Acidification of Silica (Silica purification)

To produce high-quality silica material, high-purity quartz sand is the best material option. To produce silicon powder, there are several steps involved in producing the final product. First, the Iraqi silica sand at a grade of 98% purity was ground to particles using an agate grinding jar in a Retsch PM100 planetary ball mill, volume of about 250 - 500 mg, for one hour at 400 RPM and in the presence of air. To remove surface impurities and organic contaminants surface impurities, the grind silica go through a one -hour ultrasonication process in deionized water, followed by thorough washing and drying. All natural silica minerals contain elements (C, O, N, etc.) and have other impurities (such as metals: Ca, Al, etc.) present in their structure. The second step involved removing most metal oxides (CaO, Fe_2O_3, Al_2O_3, etc.) using a pre-leach step. These metal oxides were also removed by etching with a stirrer in a 2 mol L^{-3} N HCl solution for two hours at 60 °C, followed by washing with deionized water three times to remove the etchant solution that contains iron and other metal oxides until

the suspended particles were free from acid. Finally, the suspended particles were collected using vacuum filtration and dried (for 4 hours) at 120 °C and silica in the form a white colored powder is obtained. To make high-purity nanosilica derived from sand using a method called thermal precipitation, 20 g is combined with 160 ml of NaOH as a chemical reagent of 2.5 N concentration and allowed to stir and heat until reaching PH = 14. Once the process, known as water glass, is complete; the mixture will undergo heating at very high temperatures (exceeds 400 °C or in some cases can be as high as 600 °C) for a period of 6 hours to produce fused materials such as sodium silicate (Na_2SiO_3). Following the completion of this reaction, the sodium silicate solution is separated from the solid materials using ash less filter paper (Whatman No. 41) and cooled before using 100 ml of boiling water to wash any insoluble left by the initial reaction. A solution of sodium silicate (Na_2SiO_3) is produced as defined by the Equation below [15]:

$$SiO_{2\,(sand)} + 2NaOH \rightarrow Na_2SiO_3 + H_2O \quad (1)$$

Sodium silicate solutions can be titrated with a strong amount of acid (5 N H_2SO_4), which neutralizes or titrates the solution over time while being stirred continuously. This reaction proceeds through the precipitation process, resulting in silicic acid being present in the form of amorphous silica nanoparticles that precipitate out of the solution as a white jelly; this is shown schematically in the following reaction [17]:

$$Na_2SiO_3 + H_2SO_4 \rightarrow SiO_{2\,(nanosilica)} + Na_2SO_4 + H_2O \quad (2)$$

To produce silica gel (SG), the pH value for the solution was monitored, and the titration process was stopped at a pH of 4. After the gelatin process was completed, an ammonium hydroxide solution (NH_4OH) was added until the value of the pH became 8.5. After that, it was left to age for 1 hour at room temperature. The slurry was washed with deionized water repeatedly and filtered with filter paper (Whatman No. 41, ashless). The silica gel residue was washed with 20 ml of warm (45°C) deionized water. It was allowed to cool at room temperature. Then, high-purity silica was obtained and oven-dried at 110°C for 6 hours. At this stage, the prepared silica was ready to be used as a raw material for the nano-silicon production technology.

2.3. Metallothermic-reduction technique with the Mg-Al-SiO_2 System

According to the equivalent equations 3 and 4 for both the reduction mechanisms of silica with magnesium and aluminum, the physical processes of the reactions occur on surfaces, as they both involve the reaction of solid and gas phases.

$$3SiO_{2\,(s)} + 4Al_{\,(l)} \rightarrow 3Si_{\,(s)} + 2Al_2O_{3\,(s)} \quad (3)$$

$$SiO_{2\,(s)} + 2Mg_{\,(g)} \rightarrow Si_{\,(s)} + 2MgO_{\,(s)} \quad (4)$$

To produce silicon or Al-Si alloys, magnesium and SiO_2 are heated until the mixture of magnesium melts and begins to boil. Magnetothermal reduction, having an exothermic reaction is capable of being conducted at lower temperatures (650°C) compared to aluminate (800°C), because of this, ensuring better control and consistency of the morphology of the final products as compared to those made by aluminate reductions. As a one-step, relatively low-temperature process (650°C) with the maintenance of the morphology characteristics of the original materials, magnetothermal reduction is more energy-efficient and cost-effective than carbothermic methods. Since exothermic reactions (thermal energy is released from combustion reaction without the addition of energy) provide the source of heat to perform magnetothermal reduction, and aluminum (Al) is a chemical that releases heat (combustion synthesis) during the production of magnesium-silicon composite materials using SiO_2. Excess heat generated during the conversion of Al/SiO_2 to silica particles in aluminothermic reduction produces Al/SiO_2 composites through the reaction (5) [17]:

$$3SiO_2 + 4Al \rightarrow 2Al_2O_3 + 3Si \quad (5)$$

Alumina undergoes the above changes to produce an unstable compound with silica. As a result of the reaction, mullite ($Al_6Si_2O_{13}$) is formed as well. The reduction of these two products to form silicon also involves the reduction of mullite by the addition of aluminum (Al) [17].

$$3Al_2O_3 + 2SiO_2 \rightarrow Al_6Si_2O_1 \quad (6)$$

$$8Al + 3Al_6Si_2O_{13} \rightarrow 13Al_2O_3 + 6Si \quad (7)$$

The reduction takes place at a temperature greater than 650 °C, which is a much lower temperature and has a much lower exothermic heat release than the calciothermic process [15-18].

$$SiO_{2(s)} + 2Mg_{(g)} \rightarrow 2MgO_{(s)} + Si_{(s)} \quad (8)$$

$$Si_{(s)} + 2Mg_{(g)} \rightarrow Mg_2Si_{(s)} \quad (9)$$

$$Mg_2Si + 4HCl \rightarrow 2MgCl_2 + SiH_4 \quad (10)$$

Magnesium (Mg) and aluminum (Al) are used to reduce silica depending on the Mg-Al diagram that is shown in Ellingham diagram of different oxides [15].

$$3Mg_{(g)} + Al_2O_{3(s)} \rightarrow 3MgO_{(s)} + 2Al \quad (1l)$$

The pertinent principle to the reduction of silica (SiO_2) is that the solubility of the contaminants in an alloy of silica (Si/Al/Mg) increases as the temperature increases above such alloy's eutectic temperature. A point of uniqueness about the composition of Si/Al/Mg is that no intermetallic compound is produced, as such two phases only exist, namely, the eutectic phase and pure crystalline silicon dendrite phase. The hybrid method for reducing SiO_2 is a recent and experimental method of combining inexpensive and readily available reducing agents, along with having the most basic simplicity in its mode of operation. The hybrid method employs both magnesiothermic and aluminothermic reduction methodologies up to 50% reduction ratios, thus maximizing benefits from each technique. An additional goal for using the hybrid method is to lower the reducing temperature of SiO_2 while still providing a level of purity acceptable for the reduction product. The overall concept being developed is that a modern reduction technique will provide the opportunity for redesigning traditional reduction techniques and enabling them to occur at a relatively low reduction agent to SiO_2 ratio while being conducted under mild temperature conditions. Key milestone events in developing a low cost, easily manageable reduction process for producing pure silicon are feasibility of producing acceptable high purity silicon dependent upon determining the optimal reduction agent to silica ratio, reduction time and reduction temperature. A novel hybrid technique for producing silicon nanoparticles (SiNPs) at low temperatures (about 450°C), called the hybrid reduction process, utilizes a mixture comprising 36% magnesium (Mg) and 64% aluminum (Al) added to a silica (SiO_2) reducing agent prior to mixing with alumina (Al_2O_3) powder, when applicable. Mixing is performed using only those two metals, with Mg acting as the reducing agent and aluminum (Al) acting as a reducing agent when mixed with Mg. The experimental conditions have been summarized in Table 2. To create pellets, the component powders (SiO_2 and an Al-Mg mixture) were mixed in proportions outlined above, then compacted into a mold (1 cm x 1 cm), and finally placed under an electric furnace in which they will undergo thermal reduction by heating to 550°C for 8 hour while increasing at 5°C/min with Ar gas flowing through it before being collected, ground, and then leached.

Table 2. Reduction Conditions of the Hybrid Reduction Process.

Simple Code	Ratio of (Mg, Al)%: SiO_2 (g)
S 1	(35, 65):1
S 2	(50,50):1
S 3	(70, 30):1

2.4. Leaching of reduction products

After the reduction processes by the hybrid reduction process, the reduction product is subjected to the milling process by hand-milling in a mortar. Therefore, in order to remove unwanted phases from the reduced product, multiple leaching processes by chemical materials are achieved. Hence, in order to remove the undesired phases from the reduction product, three successive chemical leaching stages are achieved after using the mortar for milling the reduction product. The first stage includes treating the product with 4N HCl for 1 hour at 60°C. The second stage is using a mixture of 4N HCl + 4N CH_3COOH as a 4:1 volume ratio at 60°C for 1 hour in a glass beaker of 250 ml, respectively. The third stage of the leaching process is carried out in a mixture of 4N HF + 4N CH_3COOH as a 1:9 ratio at 70°C for 1 hour. The final product was washed with deionized water and then separated by a centrifuge device (electric centrifuge machine laboratory practice) for 15 min at 4000 rpm with a control capacity of 20 ml x 6 tubes after each step of the chemical process. The reduction product is dried under vacuum and argon gas in the furnace for 12 hour at 120°C, such as shown in Fig. 1.

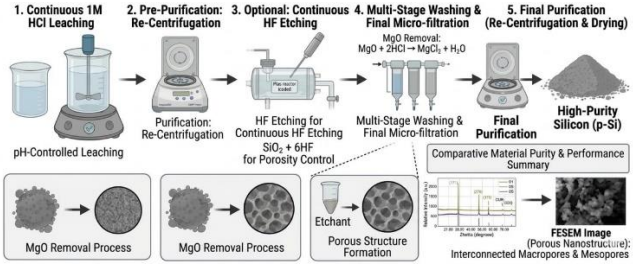

Figure 1. Schematic Diagram of the Extraction and Purification Stages of Nanostructured Silicon (P-Si).

3. Results and discussions

3.1. Silicon nanoparticles

Figures 2 to 4 of the Scanning Electron Microscope (SEM/EDS) images demonstrate three experiments (S1, S2, and S3) of high purity nano silicon powder after three leaching steps. The final product of high purity silicon powder (the silicon powder obtained) is mostly brownish color with a purity greater than 99.5% after experiment S2, as shown in Table 3. These positive and acceptable results were attributed to the proper and successful amounts of all chemicals used in extracting high purity silicon. The SEM morphology results indicated that silicon powder particle shapes were predominantly spherical but did demonstrate some agglomeration and the range of particle sizes spanned from at least nano-size to macro-size.

Table 3. EDS Analyses of the Hybrid Reduction Process.

Simple Code	Ratio of (% Mg, % Al): SiO_2 (g)	Purity of Si (from EDS) Weight %
S 1	(35, 65):1	95.5
S 2	(50,50):1	99.5
S 3	(70, 30):1	97.4

By using Scanning Electron Microscopy (SEM) in combination with Energy Dispersive Spectroscopy (EDS), one can gain greater insight into surface topology and sample elemental content. This SEM analysis of silicon nanoparticles added at a ratio [Mg, Al: SiO_2] ((35, 65):1) shows a significant change towards a refined microstructure when compared to a previous different ratio of adding where silicon was 95.5 % pure. Increasing the percent ratio of nano-silicon is considered a strong modifier of the adding ratio, leading to denser and more uniformly distributed grains. The EDS elemental analysis confirms the increased amount of nanosilicon indicating that the nano-silica has been effectively incorporated into the sample. Table 4 shows a comparison of the results obtained from the Proposed MTR (Mg-Al) method compared to other methods, which indicates the acceptable purity percentage obtained.

Table 4. Purity Analyses Compare between MTR and other Process.

Method	Source	Purity (%)	Morphology	Reference
Carbothermic	Silica Sand	98.15%.	Bulk	[1]
Magnesiothermic	Quartz	99.4%	Porous	[32]
Proposed MTR (Mg-Al)	**Iraqi Sand**	**97.47%**	**Nano-Porous**	**This Study**

Additionally, Elements Mapping by EDS as shown in Fig. 2 confirms that there is a homogeneous distribution of nanosilicon throughout the powder extracted, verifying successful distribution of nanosilica at this higher percentage ratio; this is required to achieve desired enhancements to overall performance of the material. The SEM/EDS evaluations of nanosilicon powder examples with different percentages of silica nano-particles demonstrate beneficial improvements to the microstructure. When the concentration ratios for this material increase as indicated in Table 3, refined, uniform grains, as well as improved purity from the extraction of nano silicon have occurred, as shown in Fig. 3 and 4.

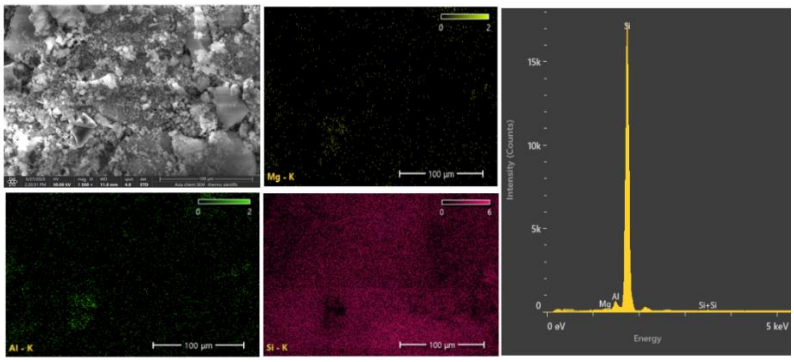

Figure 2. SEM/EDS Elemental Maps of Extracted Silicon Powder at S1.

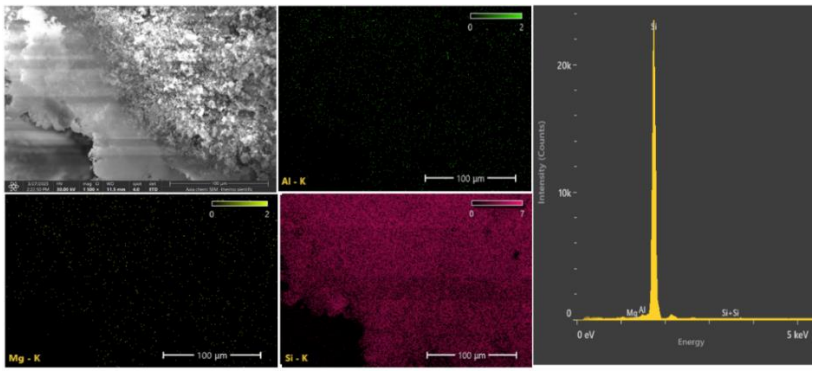

Figure 3. SEM/EDS Elemental Maps of Extracted Silicon Powder at S2.

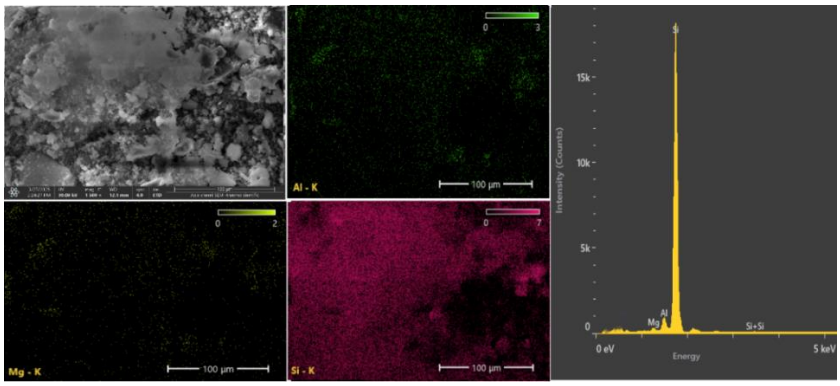

Figure 4. SEM/EDS Elemental Maps of Extracted Silicon Powder at S3.

The FE-SEM images show spherical shapes that have an uneven surface. The FE-SEM images of the products are of silicon nanoparticles. No major difference can be detected between samples S1, S2 and S3; however, when comparing these samples, it can be observed that sample S2 has a more uniform shape than either sample S1 or S3. The porosity of the silicon nanoparticles is likely due to the selective etching of the embedded MgO and Mg_2Si particles that occurred after reduction. The FE-SEM images shown in Fig. 5 are for the silicon product that was extracted after the leaching of the reduction step. It is clear from the images in Fig. 5-a, that the multiphasic product that was recovered after extraction has agglomerated. The FE-SEM images presented in Fig. 5-a, shows that although the average diameter of the silicon powder particles is approximately 49.8625 nm, the majority of the extracted silicon powder contains substantial amounts of porosity. It is also possible to see the pores in the FE-SEM images because they were etched during the leaching process. The average diameters of the silicon nanoparticles in Fig. 5-b could be estimated at approximately 30.155 nm. Also, in based on the micrograph presented in Fig. 5-c the diameters of silicon nanoparticles were approximately 58.635 nm. In silicon powdered form, its porosity contributes to increase the efficiency in removing not only metallic impurities which exist on the surface area of the particles, but also in removing interstitial elements like boron and phosphorous. This supports more efficient stages of the process and will produce an increase in final product purity.

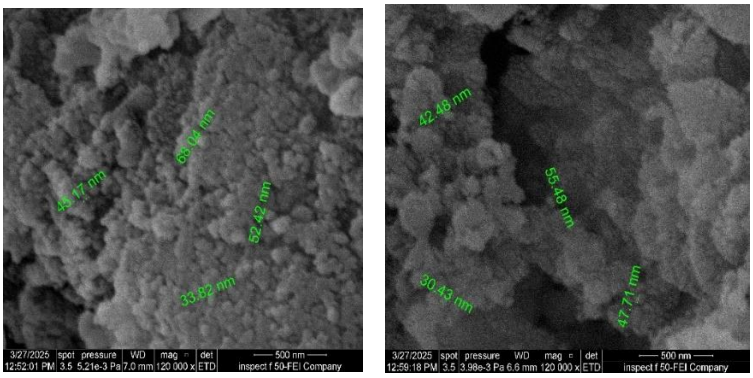

(a) (b)

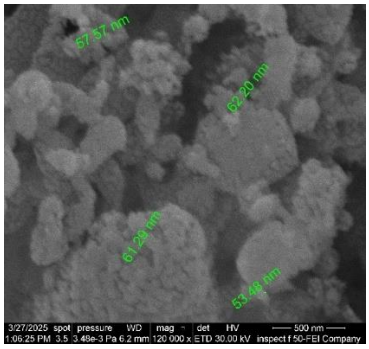

(c)

Figure 5. FE-SEM Micrographs of Extracted Product (Silicon Powder) after Refining Treatment; (a) S1, (b) S2, (c) S3.

The X-ray diffraction (XRD) patterns of the final three stages of leaching are shown in Fig. 6 as experimental results. The XRD results indicate that the as-produced silicon powder contains narrow, sharp, primary peaks, while there are also several weak peaks associated with those sharp peaks indicating a high degree of crystalline structure for the produced silicon powder versus a very low degree of crystalline structure for other products, such as impurities (showing low levels of each). All of these observations were made based on the experimental results shown in patterns 1 - 3 of Fig. 6, indicating that the reduction process was successful because amorphous silica was reduced to produce crystalline silicon. The indexed XRD peaks at $2\theta = 28.4°$, 47.3°, 56.1°, 69.1°, and 76.4° are the (111), (220), (311), (400), and (331) planes, respectively, according JCPDS cards (e.g., card #27-1402). Therefore, it may be concluded that the purity of the produced silicon and the degree of silicon purity depend significantly on the experimental conditions. The results presented in Fig. 5 indicate that silicon with the highest purity was obtained by experiments S1, S2, and S3.

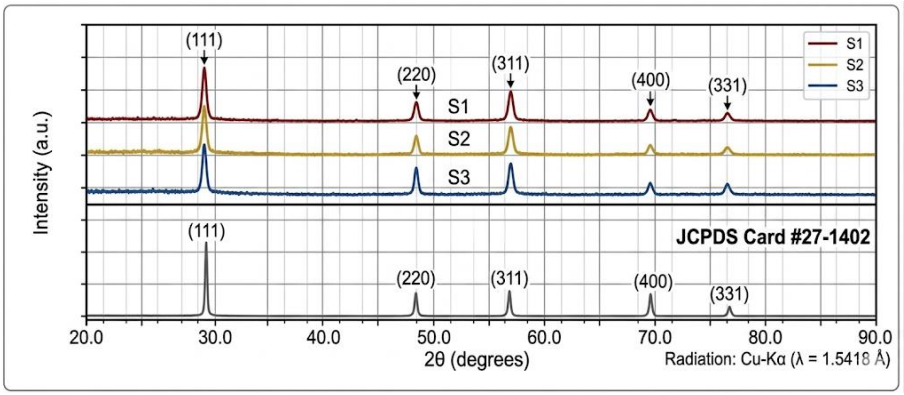

Figure 6. XRD Patterns of Reduction Product from Magnesiothermic Reaction at S 1, S 2, and S 3.

4. Conclusion

The metallothermic reduction (MTR) methodology provides a rapid and cost-effective approach for synthesizing porous silicon. This technique allows for precise control over the resulting morphologies and surface characteristics of the nanostructured material. To produce a high quality product, MTR requires the use of proper thermodynamic control and full understanding of the chemical reaction mechanisms. The use of Al/Mg alloy as the reducing agent for reducing the MTR reaction temperature will significantly enhance the energy efficiency of the process for producing porous Si. The multi-step purification process was proven to be an excellent means of totally removing all residue contaminants (including MgO and unreacted silicates) from the finished product by using [4N HCl:(HCl + CH_3COOH)] (1:4) and lastly by HF:CH_3COOH (1:9) etch, which will result in pure silicon nanoparticles containing a well-defined interconnected network of pores. The high purity and nanostructured nature of the silicon produced via the MTR method suggest its potential for future investigation as an anode material for lithium-ion batteries. The results from this work have advanced the development of this sustainable route for the production of porous Si towards commercialization; however, large-scale industrial production will still need to overcome barriers such as low Si yields and continuing

formation of secondary products. Future research will need to focus on improving reactor scalability and further suppressing the formation of by-products to achieve full commercialization of the sustainable synthesis route.

Declaration of Competing Interest

The authors declare that there are no conflicts of interest regarding the publication of this manuscript.

Funding Information

No funding was received from any financial organization to conduct this research.

Author Contributions

All authors proposed the research problem. Author Ruaa A. Salman collected recent articles, organized them in simple shapes, and designed and proposed the work. Author Asaad H. Lafta applied the experimental works. All the authors discussed the results and the final version of this paper.

Acknowledgments

The authors take this opportunity to thank the University of Technology - Iraq, specifically the College of Production and Metallurgical Engineering, for their laboratory equipment and technical support.

References

[1] P. Alonso Sanchez, K. Thangai, O. A. Oie, A. Gaarud, M. Rodriguez Gomez, V. Diadkin, J. Campo, F. H. Cova, and M. V. Blanco, "Toward the Controlled Synthesis of Nanostructured Si and SiOx Anodes for Li-Ion Batteries via SiO2 Magnesiothermic Reduction Reaction," *ACS Applied Energy Materials*, vol. 8, no. 4, pp. 2249–2259, 2025.

[2] S. A. Ajeel, K. A. Sukkar, and N. K. Zedin, "Evaluation of acid leaching process and calcination temperature on the silica extraction efficiency," *Journal of Physics: Conf. Series*, vol. 1773, p. 012014, 2021.

[3] Z. Xiuxia, Z. Jin, M. Peter, and C. Ya-Jun, "Silicon based lithium-ion battery anodes: A chronicle perspective review," *Nano Energy*, vol. 31, pp. 113-143, 2017.

[4] E. J. Anglin, L. Cheng, W. R. Freeman, and M. J. Sailor, "Porous silicon in drug delivery devices and materials," *Advanced Drug Delivery Reviews*, vol. 60, no. 11, pp. 1266–1277, 2008.

[5] Z. Huang, N. Geyer, P. Werner, J. de Boor, and U. Gösele, "Metal-Assisted Chemical Etching of Silicon: A Review," *Adv. Mater.*, vol. 23, pp. 285-308, 2011.

[6] T. Kim and J. Lee, "Silicon nanoparticles: fabrication, characterization, application and perspectives," *Micro and Nano Syst Lett*, vol. 11, p. 18, 2023.

[7] Y. Tan, T. Jiang, and G. Z. Chen, "Mechanisms and product options of magnesiothermic reduction of silica to silicon for lithium-ion battery applications," Frontiers in Energy Research, vol. 9, p. 651386, 2021.

[8] W. Deqing and S. Ziyuan, "Aluminothermic Reduction of Silica for the Synthesis of Alumina-Aluminum-Silicon Composite," *Journal of Materials Synthesis and Processing*, vol. 9, pp. 241–246, 2001.

[9] X. Ma, W. Fei, X. Zhang, J. Ji, and X. Zhou, "Preparation of Mesoporous Si Nanoparticles by Magnesiothermic Reduction for the Enhanced Reactivity," Molecules, vol. 28, no. 7, p. 3274, 2023.

[10] J. Entwistle, A. Rennie, and S. Patwardhan, "A review of magnesiothermic reduction of silica to porous silicon for lithium-ion battery applications and beyond," *Journal of Materials Chemistry A*, vol. 6, no. 38, pp. 18344-18356, 2018.

[11] J. Salonen, A. M. Kaukonen, J. Hirvonen, and V. P. Lehto, "Mesoporous silicon in drug delivery applications," *Journal of Pharmaceutical Sciences*, vol. 97, no. 2, pp. 632-653, 2008.

[12] F. Priolo, T. Gregorkiewicz, M. Galli, and T. F. Krauss, "Silicon nanostructures for photonics and photovoltaics," *Nature Nanotechnology*, vol. 9, no. 1, 2014.

[13] S. A. Ajeel, K. A. Sukkar, and N. K. Zedin, "Chemical Extraction Process for Producing High Purity Nanosilica from Iraqi Rice Husk," *Engineering and Technology Journal*, vol. 39, no. 1, 2021.

[14] Y. Tan, T. Jiang, and G. Z. Chen, "Mechanisms and Product Options of Magnesiothermic Reduction of Silica to Silicon for Lithium-Ion Battery Applications," *Frontiers in Energy Research*, vol. 9, p. 651386, 2021.

[15] S. A. Ajeel, K. A. Sukkar, and N. K. Zedin, "Extraction of High Purity Amorphous Silica from Rice Husk by Chemical Process," *IOP Conf. Series: Materials Science and Engineering*, vol. 881, p. 012096, 2020.

[16] A. Darghouth, S. Aouida, and B. Bessais, "High-purity porous silicon powder synthesis by magnesiothermic reduction of Tunisian silica sand," *Silicon*, vol. 13, no. 3, pp. 667-676, 2021.

[17] R. M. Namus, M. H. Abass, M. Alali, and N. K. Zedin, "Using green corrosion inhibitor to reduce maintenance cost for carbon steel saline water storage systems," *KOM – Corrosion and Material Protection Journal*, vol. 68, pp. 43-50, 2024.

[18] N. K. Zedin, S. A. Ajeel, and S. S. Husseinc, "Cellulose nanofibers extracted from oat husk by thermochemical processes," *AIP Conf. Proc.*, vol. 3292, p. 030005, 2025.

[19] V. A. Borisov, A. D. Kiselev, R. I. Kraidenko, and L. N. Malyutin, "The production of silicon by magnesiothermic reduction of silicon dioxide," *AIP Conference Proceedings*, vol. 2310, no. 1, p. 020048, 2020.

[20] N. K. Zedin, R. A. Salman, and A. A. Jaber, "Extraction of Cellulose Nanoparticles via Modified Thermochemical Processes from Agricultural Wastes," *IJASEIT*, vol. 12, no. 2, 2022.

[21] R. A. Salman and N. K. Zedin, "Effect Multiple Addition (TiO2 and Fly Ash) on Wear Behavior and Hardness of 2024 Al Alloy," *Materials Science Forum*, vol. 1039, pp. 201-208, 2021.

[22] N. K. Zedin, S. A. Ajeel, and K. A. Sukkar, "Nanosilicon Powder Extraction as a Sustainable Source (From Iraqi Rice husks) by Hydrothermal Process," *AIP Conf. Proc.*, vol. 2213, p. 020155, 2020.

[23] Y. Lai, J. R. Thompson, and M. Dasog, "Metallothermic Reduction of Silica Nanoparticles to Porous Silicon for Drug Delivery Using New and Existing Reductants," *Chemistry – A European Journal*, vol. 24, no. 31, pp. 7913-7920, 2018.

[24] S. A. Ajeel, K. A. Sukkar, and N. K. Zedin, "New magnesio-thermal reduction technique to produce high-purity crystalline nano-silicon via semi-batch reactor," *Materials Today: Proceedings*, vol. 42, pp. 1966-1972, 2021.

[25] R. A. Salman, S. A. Ajeel, and N. K. Zedin, "Influence of Sulphate and Chlorides Acidic Media on Mechanical and Corrosion Behavior," *IOP Conf. Series: Materials Science and Engineering*, vol. 671, p. 012153, 2020.

[26] S. Haouli, S. Boudebane, I. J. Slipper, S. Lemboub, P. Gebara, and S. Mezrag, "Combustion synthesis of silicon by magnesiothermic reduction," *Phosphorus, Sulfur, and Silicon and the Related Elements*, vol. 193, no. 5, pp. 280-287, 2018.

[27] A. W. A. Al-Razzaq, S. A. Ajeel, and N. K. Zedin, "Optimization with a Novel Hybrid Approach for Alumina Extraction from the Cement Industry Tailing," *AIP Conf. Proc.*, vol. 3303, p. 060022, 2025.

[28] Z. Favors, W. Wang, H. H. Bay, Z. Mutlu, K. Ahmed, C. Liu, M. Ozkan, and C. S. Ozkan, "Scalable Synthesis of Nano-Silicon from Beach Sand for Long Cycle Life Li-ion Batteries," *Scientific Reports*, vol. 4, no. 1, p. 5623, 2014.

[29] M. Cai, Z. Zhao, J. Qu, Q. Ma, X. Qu, L. Guo, H. Xie, D. Wang, and H. Yin, "Zincothermic reduction of silica to silicon: make the impossible possible," *Journal of Materials Chemistry A*, vol. 9, no. 34, pp. 18630-18638, 2021.

[30] A. Darghouth, S. Aouida, and B. Bessais, "High Purity Porous Silicon Powder Synthesis by Magnesiothermic Reduction of Tunisian Silica Sand," *Silicon*, vol. 13, no. 3, pp. 667-676, 2021.

[31] D. Tandersen, Y. A. Sata, U. A. Nizhamul, P. Yudaprawira, A. L. Pambudi, W. D. Sulakso, and Z. Zulhan, "Extraction of Silicon From Silica Sand by Carbothermic Reduction in Mini DC-EAF," *in E3S Web of Conferences*, vol. 543, p. 02006, 2024.

[32] F. Farirai, M. Ozonoh, T. C. Aniokete, O. Eterigho-Ikelegbe, M. Mupa, B. Zeyi, and M. O. Daramola, "Methods of extracting silica and silicon from agricultural waste ashes and application of the produced silicon in solar cells: a mini-review," *International Journal of Sustainable Engineering*, vol. 14, no. 1, pp. 57–78, 2021.